

## SUPPLEMENTARY INFORMATION

### Molecular mechanisms for protein-encoded inheritance

Jed J.W. Wiltzius\*, Meytal Landau\*, Rebecca Nelson\*, Michael R. Sawaya\*, Marcin I. Apostol, Lukasz Goldschmidt, Angela B. Soriaga, Duilio Cascio, Kanagalaghatta Rajashankar, David Eisenberg

\* Contributed equally

### Supplementary Figures

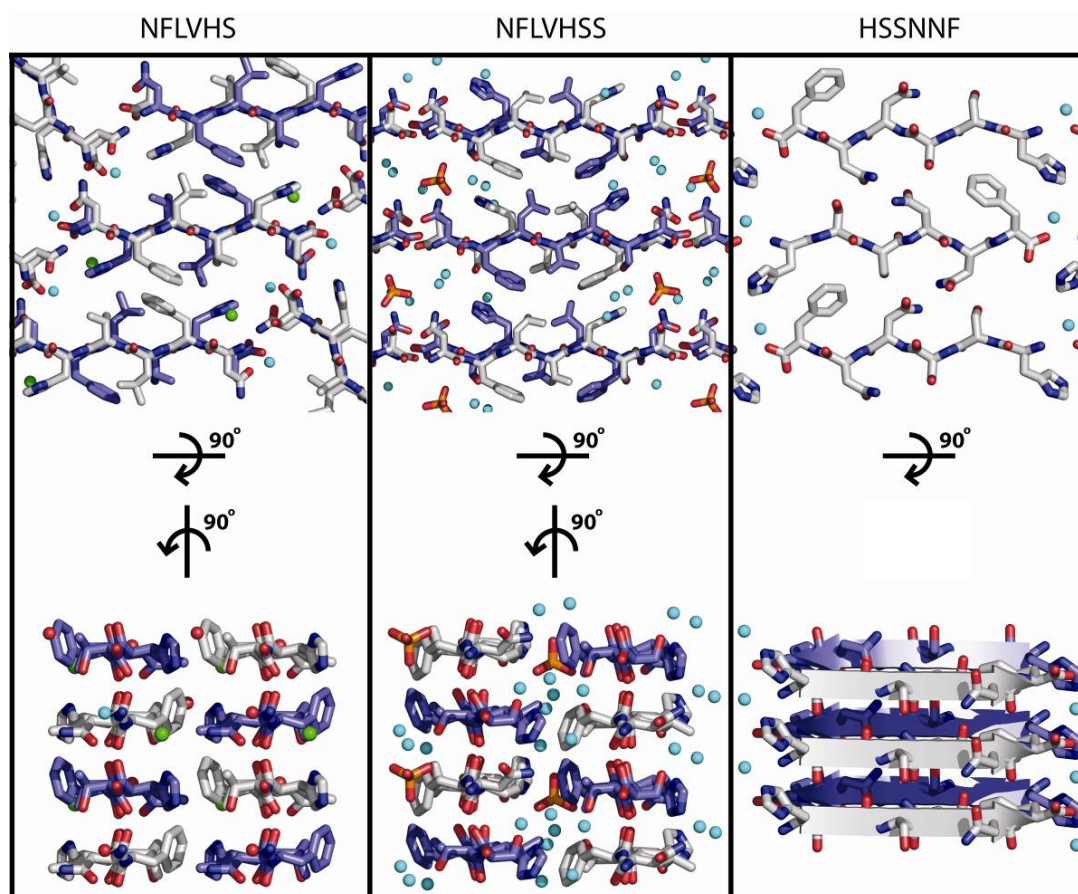


**Figure 1.** The microcrystal structures of steric zippers formed by segments NFLVHS, NFLVHSS, and HSSNNF of IAPP. Water molecules are shown as aqua spheres. Both NFLVHS and the NFLVHSS segments are antiparallel with respect to  $\beta$ -strands within a  $\beta$ -sheet. A chloride ion (shown as a green sphere) is coordinated between histidine residues of every other  $\beta$ -strand within each  $\beta$ -sheet of NFLVHS. A sulfate ion lies within the NFLVHSS structure. The structure of HSSNNF reveals parallel  $\beta$ -strands within  $\beta$ -sheets and dry, identical interfaces between each pair of sheets. The  $\beta$ -strands between adjacent  $\beta$ -sheets are in the same plane for NFLVHS and NFLVHSS, whereas they are staggered in HSSNNF.

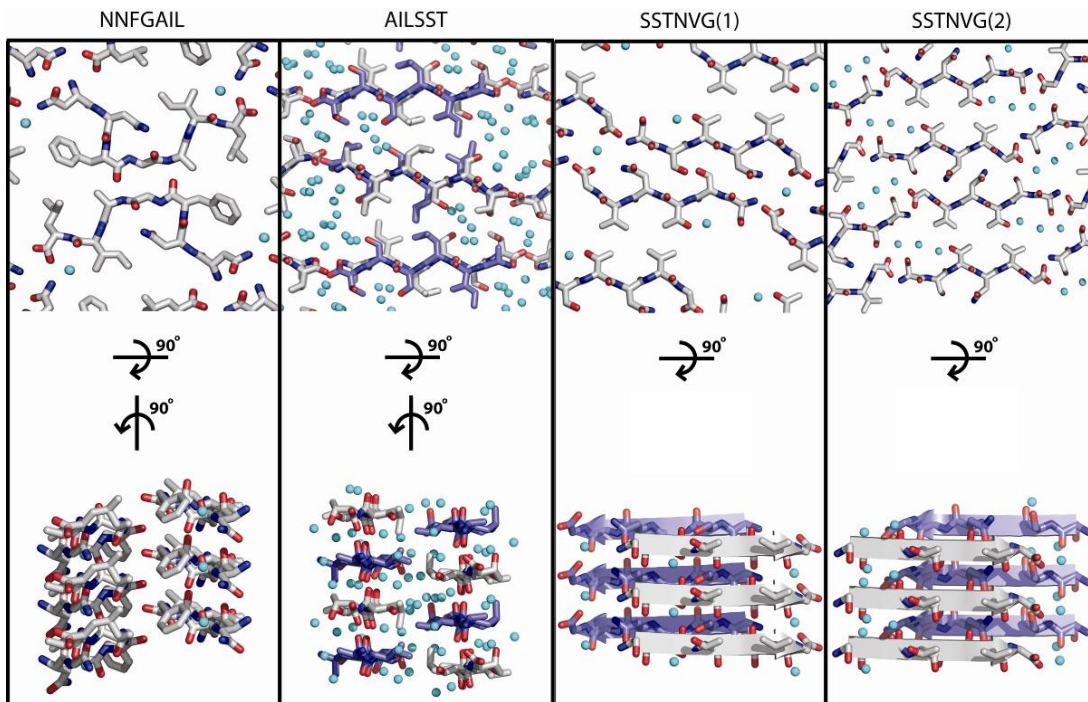


**Figure 2.** The microcrystal structures of steric zippers formed by segments from residues 21-33 from IAPP. The NNFGAIL and SSTNVG structures as published previously<sup>1</sup>. The structure of the AILSST segment reveals antiparallel  $\beta$ -strands within adjacent  $\beta$ -sheets. The  $\beta$ -strands between adjacent  $\beta$ -sheets are in the same plane. The structure of the second packing of SSTNVG shows a shift in the registry between adjacent  $\beta$ -sheets. The center of the interface is now Asn31, rather than Ser29.

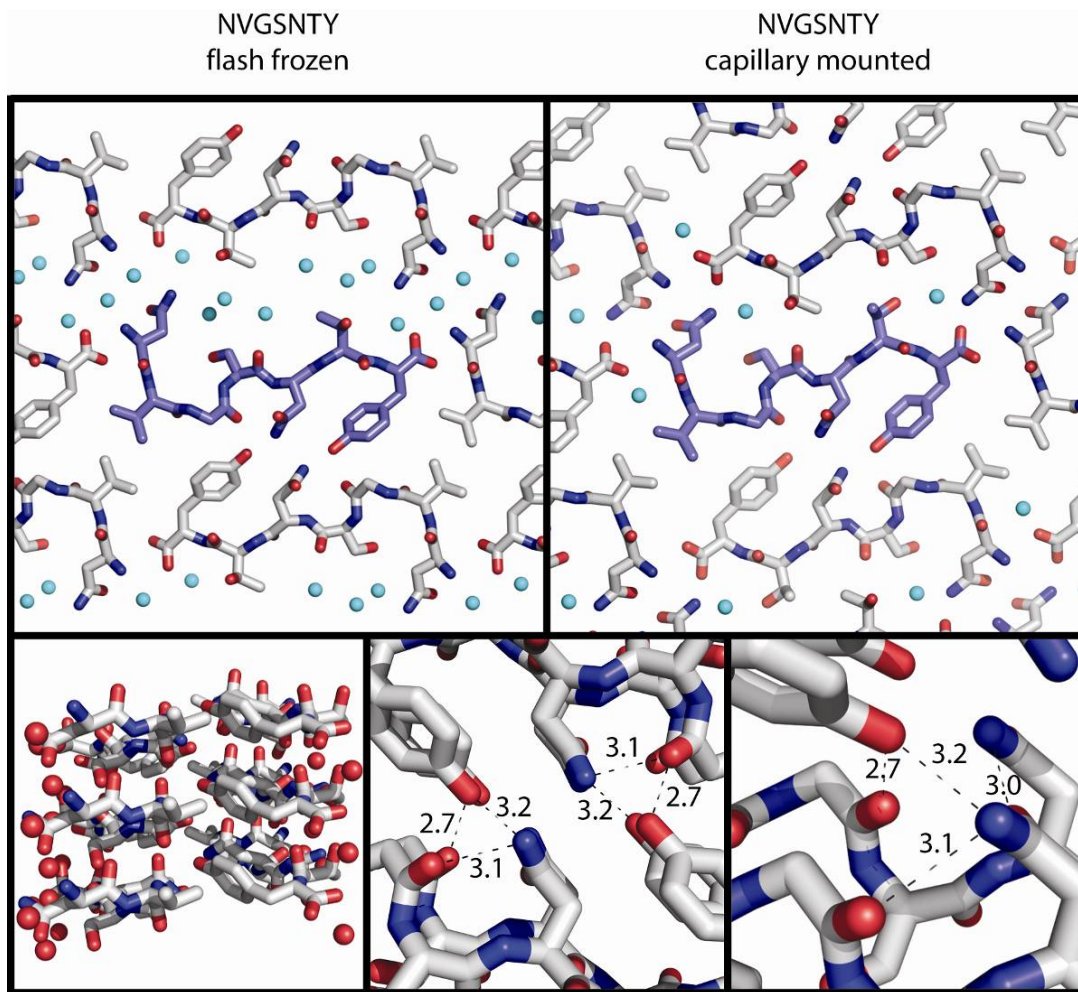


**Figure 3.** The preparation of microcrystals derived from amyloid-like fibrils influences the hydration state of the wet interface. The structures of NVGSNTY determined in identical conditions (see Supplemental Methods) were solved by either flash freezing the crystals in liquid nitrogen (top left) or mounting dry crystals on glass capillaries (top right). The flash frozen sample shows more water molecules at the wet interface. Importantly, the dry interface at the center of the structure remains identical. This dry interface reveals an intricate hydrogen-bonding network, rather than closely interdigitated sidechains.

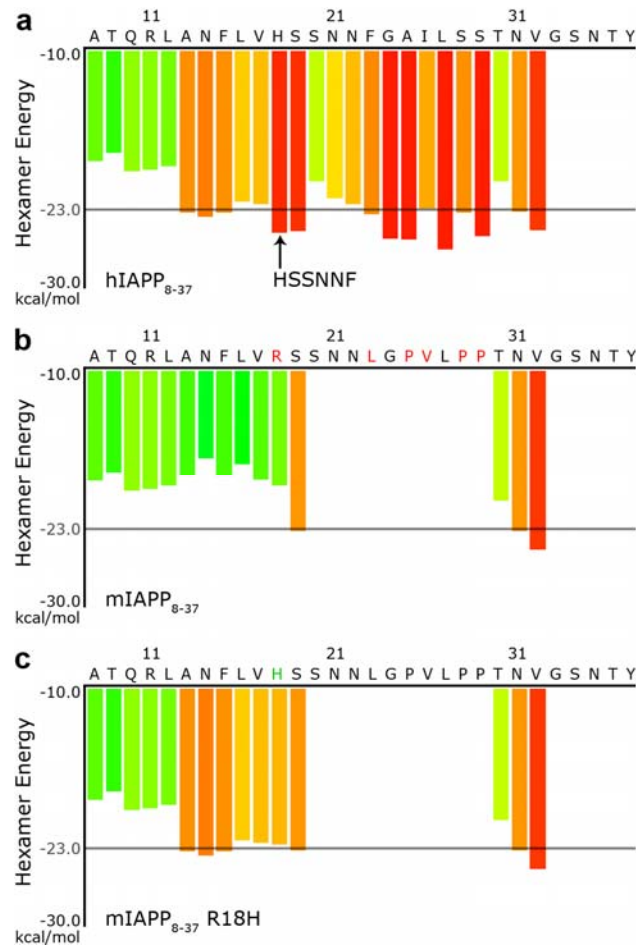


**Figure 4.** The 3D profile method<sup>2</sup> provides a computational explanation for the aggregation of mIAPP R18H. **a**, The scan of computed energies versus sequence for segments of human IAPP reveals several aggregation-prone hexameric segments spanning from residue 13 all the way through the final hexamer at position 32. **b**, Mouse IAPP scores poorly due to the Arg residue at position 18 and the Pro residues at positions 25, 28, and 29. The final hexamer at position 32 still scores well because these residues are the same in the mouse and human constructs. The upstream proline residues may prevent this segment from forming a cross-β, steric-zipper spine in the full-length mouse construct. **c**, The mIAPP R18H protein can form fibrils because these segments contain His18, permitting the formation of a steric zipper spine incorporating this residue.

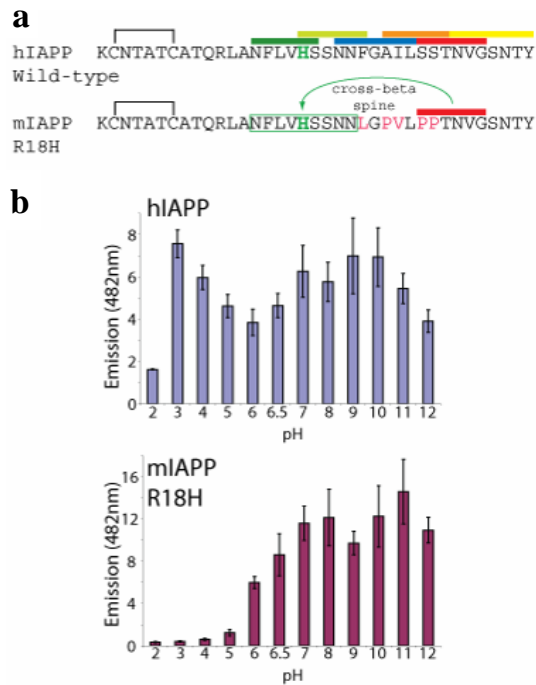


**Figure 5.** Fibrils of the mIAPP R18H construct contain a cross- $\beta$  spine outside the C-terminal putative amyloidogenic domain. **a**, The primary structure diagram above shows color-coded segments that form both fibrils and microcrystals within hIAPP. The Pro residues within mIAPP R18H at positions 28 and 29 prevent this region from forming a cross- $\beta$  spine. A segment composed of PPTNVG is incapable of forming fibrils or microcrystals (data not shown). **b**, Fiber formation of hIAPP as a function of pH shows that hIAPP forms fibrils regardless of pH. The fiber formation capability of mIAPP R18H has an inflection point near the pKa of His, suggesting a direct involvement of this position in the fiber formation of this construct.



## Supplementary Table

**Supplementary Table 1. Features of the steric zipper (dry interface) of microcrystals derived from fibril-forming proteins.**

	Strand Orientation	Area buried <sup>a</sup> (Å <sup>2</sup> )		Shape complementarity <sup>b</sup>		Inter sheet distance <sup>c</sup> (Å)		Rosetta score <sup>d</sup> (kcal mol <sup>-1</sup> )		PDB code
<b>NNQNTF<sup>e</sup></b>	parallel	726	516	0.77	0.85	7.7	8.4	-22.5	-21.4	3FVA
<b>VQIVYK Form 1</b>	parallel	378		0.76		9.9		-25.2		2ON9
<b>VQIVYK Form 2</b>	parallel	256		0.89		8.7		-25.9		3FQP
<b>NFLVHS</b>	Antiparallel	287		0.78		9.9		-21.8		3FR1
<b>NFLVHSS</b>	Antiparallel	265		0.57		10.8		-24.7		3FTH
<b>HSSNNF</b>	parallel	491		0.83		8.2		-22.5		3FPO
<b>AILSST<sup>f</sup></b>	Antiparallel	343		0.55		9.8		-23.6		3FOD
<b>SSTNVG Form 1</b>	parallel	474		0.86		5.8		-25.4		3DG1
<b>SSTNVG Form 2</b>	parallel	444		0.80		5.7		-23.3		3FTR
<b>NVGSNTY Form 1</b>	parallel	432		0.87		9.6		-27.1		3FTK
<b>NVGSNTY Form 2</b>	parallel	474		0.86		9.7		-25.9		3FTL

<sup>a</sup>The Area buried was calculated using areaimol<sup>3,4</sup> with a probe radius of 1.4Å. The difference between the accessible surface areas of one β-strand alone and within the steric zipper structure constitutes half of the reported area buried.

<sup>b</sup>Lawrence and Colman's shape complementarity index<sup>5</sup>

<sup>c</sup>Sheet-to-sheet distances were calculated as the shortest distance between two least squares lines fitted to the main chain atoms of two opposing strands in the dry interface. The lines were projected onto a plane normal to the "fibril axis".

<sup>d</sup>The Rosetta score was calculated as described in the Methods (main text).

<sup>e</sup>NNQNTF structure contains two different polymorphs. The numbers of the left side correspond to the steric zipper of the polymorph shown on the right panel of Figure 1d.

<sup>f</sup>The steric zipper of AILSST contains water molecules, thus is not a completely dry interface. The calculations for the area buried, shape complementarity and inter sheet distance were performed using the deposited PDB structures, while the Rosetta score is calculated for a minimized structure (repacking of the side chains) with added hydrogens.

## Supplementary Methods

In this paper, we report 9 new crystals structures of: NNQNTF, NFLVHS, NFLVHSS, HSSNNF, AILSST, two crystals forms of NVGSNTY, SSTNVG Form 2, and VQIVYK Form 2. The crystallization conditions are described below. Note that NNQNTF displays two unique steric zippers (Fig. 1 of the main text), thus our data present an overall of 10 new and unique steric zippers. The two polymorphic forms of NNQQ<sup>6</sup>, as well as SSTNVG Form 1 (ref. 1), and VQIVYK Form 1 (ref. 6), were previously reported. Additional structures of SSTNVG Form 2 and VQIVYK Form 2 were determined out of various crystallization conditions. Some of these structures show different number of hetero atoms. The details are provided below.

### Crystallizing conditions:

**NNQNTF:** Hanging-drop vapor diffusion; drop was a mixture of segment solution (30 mg ml<sup>-1</sup> NNQNTF in 20mM BisTris) and reservoir solution (0.2M Ammonium Sulfate, 0.1M Tris pH 8.5, 25% PEG 3350). The structure was solved to 1.45Å resolution and contained one segment and two water molecules in the asymmetric unit.

**NFLVHS:** Hanging-drop vapor diffusion; drop was a mixture of segment solution (20 mg ml<sup>-1</sup> segment in water) and reservoir solution (0.18M MgCl<sub>2</sub>, 0.09M HEPES pH 7.5, 27% isopropanol, and 10% glycerol). The structure was determined to 1.85Å resolution and contained one segment, one water molecule and one chloride ion in the asymmetric unit.

**NFLVHSS:** Hanging-drop vapor diffusion; drop was a mixture of segment solution (20 mg ml<sup>-1</sup> segment in water) and reservoir solution (1.5 M ammonium sulfate, 0.1 M sodium acetate trihydrate pH 4.6). The structure was determined to 1.8 Å resolution and contained two segments, six water molecules and one sulfate ion in the asymmetric unit.

**HSSNNF:** Hanging-drop vapor diffusion; drop was a mixture of segment solution (20 mg ml<sup>-1</sup> segment in water) and reservoir solution (0.1M Tris HCl pH 8.5, 8% PEG 8000). The structure was determined to 1.5Å resolution and contained one segment, and one water molecule in the asymmetric unit.

**AILSST:** Hanging-drop vapor diffusion; drop was a mixture of segment solution (40 mg ml<sup>-1</sup> segment in water) and reservoir solution (0.2M MgNO<sub>3</sub> pH 5.9, 20% PEG 3350). The structure was determined to 1.4Å resolution and contained eight segments, and 67 water molecules in the asymmetric unit.

**NVGSNTY:** Hanging-drop vapor diffusion; drop was a mixture of segment solution (40 mg ml<sup>-1</sup> segment in water) and reservoir solution (0.1M HEPES pH 7.5, 25% PEG 3350). Two crystals of NVGSNTY were grown in the above identical conditions but prepared for data collection by either flash freezing the crystals in liquid nitrogen or mounting dry crystals on glass capillaries. The crystal structure obtained from flash frozen sample was determined to 1.5Å resolution and contained one segment and five water molecules in the asymmetric unit (Form 1). The structure obtained from mounting dry crystals on glass capillaries was determined to 1.6Å resolution and contained two segments and three water molecules in the asymmetric unit (Form 2).

**SSTNVG (Form 1 space group C2):** described previously<sup>1</sup> (PDB code 3DG1). Hanging-drop vapor diffusion; drop was a mixture of segment solution (2 mg ml<sup>-1</sup> SSTNVG in water) and reservoir solution (30% v/v MPD). The structure was solved to 1.65Å resolution and contained one segment and two water molecules in the asymmetric unit.

**SSTNVG (Form 2 space group P212121):** Hanging-drop vapor diffusion; drop was a mixture of segment solution (20 mM SSTNVG in water in the presence of 2 mM rifamycin SV sodium salt and 0.5 mM ascorbic acid) and reservoir solution (20% w/v PEG-3000, 0.1M HEPES pH 7.5, 0.2M NaCl). The structure was solved to 1.6Å resolution and contained one segment and three water molecules in the asymmetric unit.

Note: The same crystal packing was also obtained using the following crystallization conditions:

Hanging-drop vapor diffusion; drop was a mixture of 20 mM SSTNVG in 19% ethanol in the presence of 2mM curcumin, and reservoir solution (0.1M HEPES pH 7, 30% Jeffamine M-600 pH 7). The structure was determined to 1.85Å resolution and contained one segment and three water molecules in the asymmetric unit.

**VQIVYK (Form 1 space group P21):** Described previously<sup>6</sup> (PDB code 2ON9). Hanging-drop vapor diffusion; drop was a 1:1 mixture of segment solution (30 mg ml<sup>-1</sup> VQIVYK in water) and reservoir solution (0.2 M ammonium acetate, 0.1M Na HEPES pH 7.5, 45% v/v MPD). The structure was solved to 1.5Å resolution and contained two segments and seven water molecules in the asymmetric unit.

**VQIVYK (Form 2 space group C2):** Hanging-drop vapor diffusion; drop was a 1:2-2:1 mixture of segment solution (10mM SSTNVG in 80% DMSO in the presence of 1 mM perphenazine) and reservoir solution (14% iso-propanol, 0.07 M HEPES-Na pH 7.5, 0.14 M Sodium Citrate, 30% Glycerol). The structure was solved to 1.5Å resolution and contained one segment and one water molecule in the asymmetric unit.

**Note** – the same crystal packing was also obtained using the following crystallization conditions; all contained one segment in the asymmetric unit:

1. Hanging-drop vapor diffusion; drop was a 1:2-2:1 mixture of segment solution (10mM VQIVYK in 60% DMSO with and without 1 mM or 2 mM curcumin) and reservoir solution (0.1M Tris HCl pH 8.5, 70% v/v MPD). The structure of the crystals grown in the presence of 1mM Curcumin was determined to 1.7 Å resolution and contained one water molecule in the asymmetric unit. The structure of the crystals grown in the presence of 2 mM curcumin was determined to 1.7Å resolution and contained no water molecules. The structure of the crystals soaked with 1mM Curcumin was solved to 1.5 Å resolution and contained one water molecule in the asymmetric unit. The structure of the crystals grown without Curcumin was determined to 1.7Å resolution and contained one water molecule in the asymmetric unit.

2. Hanging-drop vapor diffusion; drop was a 1:2-2:1 mixture of segment solution (10mM VQIVYK in water in the presence of 1mM 2-Methoxy-4-methylphenol (Creosol)) and reservoir solution (1M succinic acid pH 7, 0.1M HEPES pH 7, 1% w/v Polyethylene glycol monomethyl ether 2,000). The structure was determined to 1.7 Å resolution and contained one water molecule in the asymmetric unit.

3. Hanging-drop vapor diffusion; drop was a 1:2-2:1 mixture of segment solution (10 mM VQIVYK in 40% DMSO in the presence of 1 mM juglone) and reservoir solution (0.1M Tris.HCl pH 8.5, 70% v/v MPD). The structure was determined to 1.8Å resolution and contained one water molecule in the asymmetric unit.

4. Hanging-drop vapor diffusion; drop was a 1:2-2:1 mixture of segment solution (10 mM VQIVYK in 10% DMSO in the presence of 1 mM neocuproine) and reservoir solution (0.1M Tris pH 8, 20% v/v MPD). The structure was determined to 1.8Å resolution and contained no water molecules in the asymmetric unit.

5. Hanging-drop vapor diffusion; drop was a 1:2-2:1 mixture of segment solution (10mM VQIVYK in water in the presence of 1 mM thioflavin S) and reservoir solution (1M succinic acid pH 7.0, 0.1 M HEPES pH 7, 1% w/v Polyethylene glycol monomethyl ether 2,000). The structure was determined to 1.5Å resolution and contained one glycerol molecule in the



asymmetric unit.

6. Hanging-drop vapor diffusion; drop was a 1:2-2:1 mixture of segment solution (10 mM VQIVYK in 25% ethanol in the presence of 2 mM curcumin) and reservoir solution (0.1M MMT buffer pH 8, 30% PEG 1500). The diffraction data from this condition was merged with data from additional crystal, also prepared using hanging-drop vapor diffusion: drop was a 1:2-2:1 mixture of segment solution (10mM VQIVYK in 25% ethanol in the presence of 2mM Curcumin) and reservoir solution (1M succinic acid pH 7.5, 0.1M HEPES pH 7.5, 1% w/v Polyethylene glycol monomethyl ether 2,000). The structure was determined to 2.1Å resolution and contained one water molecule in the asymmetric unit.

### Structure determination and refinement

X-ray diffraction data were collected at beamline 24-ID-E of the Advanced Photon Source, Argonne National Laboratory; wavelength of data collection was 0.9792. NNQNTF diffraction data were collected at European Synchrotron Radiation Facility, beamline ID-13; wavelength of data collection was 0.9465 Å. Data were collected at 100 K.

Molecular replacement solutions for all segments were obtained using the program Phaser<sup>7</sup>. The search models consisted of available structures of different crystal forms of the same segment, or geometrically idealized  $\beta$ -strands with side chain conformations modeled as the most frequently observed rotamer defined in the graphics program O<sup>8</sup>. Crystallographic refinements were performed with the program Refmac<sup>9</sup>. Model building was performed with Coot<sup>10</sup> and illustrated with PyMOL<sup>11</sup>. There were no residues that fell in the disallowed region of the Ramachandran plot.

### Supplementary References

1. Wiltzius, J. J. *et al.* Atomic structure of the cross- $\beta$  spine of islet amyloid polypeptide (amylin). *Protein Sci.* **17**, 1467-74 (2008)
2. Thompson, M. J. *et al.* The 3D profile method for identifying fibril-forming segments of proteins. *Proc. Natl. Acad. Sci. U. S. A.* **103**, 4074-8 (2006)
3. Lee, B. & Richards, F. M. The interpretation of protein structures: estimation of static accessibility. *J. Mol. Biol.* **55**, 379-400. (1971)
4. Saff, E. B. & Kuijlaars, A. B. J. Distributing many points on a sphere. *Math. Intelligencer* **19**, 5-11 (1997)
5. Lawrence, M. C. & Colman, P. M. Shape complementarity at protein/protein interfaces. *J. Mol. Biol.* **234**, 946-50. (1993)
6. Sawaya, M. R. *et al.* Atomic structures of amyloid cross-beta spines reveal varied steric zippers. *Nature* **447**, 453-7 (2007)
7. McCoy, A. J. *et al.* Phaser crystallographic software. *J. Appl. Cryst.* **40**, 658-674 (2007)
8. Jones, T. A., Zou, J. Y., Cowan, S. W. & Kjeldgaard. Improved methods for building protein models in electron density maps and the location of errors in these models. *Acta Crystallogr. A* **47 (Pt 2)**, 110-9 (1991)
9. Murshudov, G. N., Vagin, A. A. & Dodson, E. J. Refinement of macromolecular structures by the maximum-likelihood method. *Acta Crystallogr. D Biol. Crystallogr.* **53**, 240-55 (1997)
10. Emsley, P. & Cowtan, K. Coot: model-building tools for molecular graphics. *Acta Crystallogr. D Biol. Crystallogr.* **60**, 2126-32 (2004)
11. DeLano, W. L. DeLano Scientific, San Carlos, CA, USA. (2002)